신경망기법을 사용한 부분구조추정법

Structural Identification Using Substructural and Neural Network Techniques

방 은 영* 윤 정 방**
Bahng, Eun-Young Yun, Chung-Bang

요 지

본 논문에서는 역전파학습에 의한 신경망기법을 사용하여 구조물의 미지계수를 추정하는 기법을 연구하였다. 대형구조물의 경우 계측 또는 추정하여야 하는 자유도의 수가 많으므로 인하여 구조계수를 추정하는 데에는 많은 어려움이 존재한다. 이러한 어려움을 극복하기 위하여 부구조추정법과 부행렬계수를 사용하여 추정하고자 하는 미지계수의 수를 효율적으로 줄일 수 있도록 하였다. 구조물의 고유주파수 및 모드형상 등의 모드계수를 신경망의 입력자료로 사용하였으며, 추정하고자하는 부재의 부행렬계수를 신경망의 출력자료로 사용하였다. 입력자료로 사용되는 모드계수에 포함되어 있는 계측오차 및 신호처리오차의 영향을 줄이기 위하여, 신경망의 학습과정에서 노이즈를 첨가하는 기법을 사용하였다. 일반적인 형태의 자켓구조물을 대상으로 수치해석을 수행함으로써 제안기법의 대형구조계에 대한 적용성을 검증하였다.

핵심용어 : 신경망 기법, 부분구조추정법, 부행렬계수, 노이즈 첨가 학습

Abstract

A method is presented for estimating unknown parameters of offshore structures using a backpropagation neural network. Several techniques are employed to overcome the issues associated with a large number of degrees of freedom. They are the substructural identification and the submatrix scaling factor. The modal data such as natural frequencies and mode shapes are used as input to the neural network for effective element-level identification particularly for the case with incomplete measurement of modal data. A numerical example analysis on a jacket-type offshore structure is presented to illustrate the proposed procedure and to demonstrate the effectiveness of the method.

Keywords : *neural network techniques, substructural identification, submatrix scaling factor, noise injection learning*

1. INTRODUCTION

In relation to the problems of damage detection and maintenance of old structures, estimation of element-level stiffness parameters becomes an increasingly important issue (Na-

* 정회원·Univ. of California, Irvine 토목환경공학과, 박사 후 연구원 과정
** 정회원·한국과학기술원 토목공학과, 교수

• 이 논문에 대한 토론을 1999년 3월 31일까지 본 학회에 보내주시면 1999년 6월호에 그 결과를 게재하겠습니다.

tke and Yao 1986, Hong and Yun 1993, Ghanem and Sinozuka 1995). In recent years, the pattern matching techniques using neural networks have drawn considerable attention in the field of damage assessment. Several researchers have dealt with neural network approaches for damage estimation of structural models with a small degrees-of-freedom (Wu et al 1992, Tsou and Shen 1994, Pandey and Barai 1995). Although their results look promising, some issues related to a large number of degrees of freedom have to be resolved, before it can be a truly viable method for structural identification. In this study, the neural network-based approach is extended to the estimation of structural parameters of a complex structural system such as a jacket-type offshore structure. Several techniques, such as substructural identification (Koh et al 1991; Oreta and Tanabe 1994; Yun and Lee 1995), submatrix scaling factor (Lim 1990), and modal strain energy (Lim 1991) are employed to overcome the issues associated with a large number of unknowns. A numerical example analysis on a jacket-type offshore structure is presented to demonstrate the effectiveness of the proposed method.

2. NEURAL NETWORK-BASED STRUCTURAL IDENTIFICATION

Studies on neural networks have been motivated to imitate the way that the brain operates (Haykin 1994). It has recently drawn considerable attention in various fields of science and technology, such as character recognition, electro-communication, image processing, and industrial control problems. Many researchers have developed various neural network models for different purposes (Hush and Horne 1993). In this study, a model called backpropagation neural network (BPNN) is used for structural identification. The basic strategy for developing a neural network-based approach to identification of a structural system is to train the BPNN to recognize the element-level structural parameters from measurement data on the structural behavior, such as natural frequencies and vibration mode shapes.

2. 1 Substructural Identification and Submatrix Scaling Factor

For the identification of a structure with many unknowns, it is not practical to identify all of the parameters in the structure at a time, because most of the identification techniques require expensive computation that would be prohibitive as the number of unknown parameters increases. Several researches were reported on identification of a part of a structure so as to reduce the size of the system under consideration. Those works were based on the reasoning that the expected damage of a structure occurs at several critical locations, hence it is more reasonable to concentrate the identification at critical locations of the structure.

The local-identification method is generally based on substructuring, in which the structure is subdivided into several substructures and the identification is carried out on a substructure at a time. In the present study, a substructure to be identified is called the internal substructure, while the others are called the external substructures as shown in Fig 1. Since the parameters to be estimated are limited to a substructure, it is expected that the numerical problems such as divergence or falling into local minima may be avoided. Another advantage is that this approach requires measurement data only on the substructure of interest, instead of on the whole structure.

The number of parameters to be estimated are kept reasonably small for successful identification of a structure. Reduction of parameters improves the results of the identification and minimize the required measurement data. For the purpose of efficient parameterization of the structure, the submatrix scaling technique is adopted in this study (Lim 1990). Using the submatrix scaling technique, the stiffness matrix of the system can be described by introducing the submatrix scaling factors (SSF) corresponding to the element level stiffness matrices as

$$K = \sum_{j=1}^{p} s_j K_j^o \tag{1}$$

where K is the stiffness matrix of the structure in the present condition, K_j^o is the jth reference value of the stiffness submatrix for the jth element transformed into the global coordinates, which means the undamaged stiffness submatrix or the stiffness submatrix estimated by the previous identification, s_j is the jth SSF, and p is the total number of submatrices. Since the submatrix can represent a single element or a group of elements of the structure with the known geometry, material properties, and boundary conditions, a significant reduction of the unknown parameters can be achieved by grouping the structural elements with the same stiffness characteristics. Then, the identification of the stiffness matrix is performed by estimating the submatrix scaling factors instead of all of the stiffness matrix coefficients. Direct identification of the stiffness matrix coefficients may face characteristics which violate the basic properties of the stiffness matrix; such as symmetry and positive definiteness. However, the use of the SSF's described in Eq. (1) can avoid such problems.

2.2 Modal Data as Input to Neural Networks

A way of choosing the patterns representing the characteristics of the structure, which will be used as input to the neural network, is one of the most important subjects in this approach. Several researchers have used the various input patterns suitable for their purpose. For example, Wu et al. used the frequency spectrum for each DOF of the example structure for damage estimation (Wu et al 1992). This input has an advantage that does not need the modal parameter identification from measurements. Nonetheless, to characterize these spectral properties, tremendous amount of sampling data is required. Accordingly, a large number of input nodes is needed, which may reduce the efficiency and accuracy of the training process. Tsou and Shen used the dynamic residual vector that can be obtained from the modal data (Tsou and Shen 1994). It provides a simple and effective way to detect the damage and the length of the input pattern can be reduced significantly compared with the spectrum data. However, it still has the restriction that the modes should be measured at every finite element DOF's. In reality, the modes obtained from a typical modal survey are generally incomplete in the sense that the mode vector coefficients are available only at the test DOF's. Therefore, it is desirable to use the input patterns which are more suitable for the case with partial measurement data

Using the substructuring technique and referring to Fig. 1, the mode shape matrix can be partitioned as

$$\Phi = \begin{bmatrix} \Phi_1^L & \Phi_1^H \\ \Phi_2^L & \Phi_2^H \\ \Phi_3^L & \Phi_3^H \end{bmatrix} \qquad (2)$$

where the subscripts 1, 2, and 3 denote substructures, substructure 2 being the internal substructure ; and the superscripts L and H represent lower and higher modes, where only the lower modes are generally used for the structural identification. Rewriting the ith mode in the partitioned modal matrix Φ_2^L as $\tilde{\varphi}_i$ for simplicity, the input pattern can be defined as

$$InputPatternVector =$$

$$(f_i,\ \varphi_{1,i} \cdots \varphi_{n,i}),\ i=1,\ \ldots,\ m\} \qquad (3)$$

where f_i is the ith natural frequency, $\tilde{\varphi}_{ji}$ denotes the jth component of which is normalized as $\tilde{\varphi}_i^T \varphi_i = 1,\ n$, n is the number of DOF's for Substructure 2, and m is the number of modes to be included in the identification.

A useful relationship between the submatrix for the element stiffness and the modes may be obtained by examining the strain energy of each submatrix with respect to the modes (Lim 1990). The modal strain energy distribution among the stiffness submatrices for the ith mode can be evaluated as

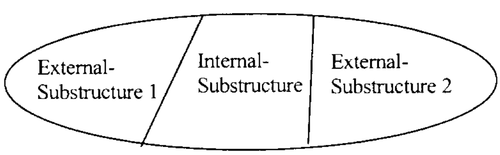

Fig. 1. Substructuring for localized identification.

$$\beta_{ji} = \frac{\varphi_i^T \cdot K_j \cdot \varphi_i}{\varphi_i^T \cdot M \cdot \varphi_i \cdot \omega_i^2} \qquad (4)$$

where β_{ji} is the modal strain energy (MSE) coefficient of submatrix K_j in the ith mode, K_j is the stiffness submatrix for the jth element transformed into global coordinates, φ_i is the ith mode shape, and ω_i is the ith circular natural frequency. The submatrices containing large values of the MSE's for a mode indicate that the corresponding structural elements are major load carrying elements for the particular mode. Stiffness changes in those elements will cause significant changes in the frequency and mode shape. Hence, detection of the stiffness changes may be more effective by examining the modal data for those elements. On the other hand, the structural elements having negligible MSE's reflect that it would be difficult to detect the stiffness changes in those elements using the corresponding modal data. They are used to determine which modes have better information for structural identification.

2.3 Generation of Training Patterns

Since the neural network-based structural identification is highly dependent on the training patterns, it is very important to prepare well-examined data sets. Consequently, it is required that the number of training patterns must be large enough to represent the structural system properly. However, for computational efficiency, it must be reasonably small, because most of the computational time for this method is required for preparing the training patterns and training the network. When the number of the unknown parameters is N and each parameter has M sampling points, the size of whole population is M^N. Accordingly, a sparse sampling algorithm such as Latin hypercube is introduced in this study (Press et al 1992). The Latin hypercube sampling makes the required number of samples reduced from M^N to M.

The training patterns for the proposed neural network-based method consist of the modal data as input and the corresponding SSF's as output. To generate training patterns, a series of eigen analyses is to be performed. However, iterative computations of eigenvalue problems for complex structures may be very expensive. Thus, the fixed-interface-component-mode-synthesis (CMS) method incorporating the substructuring technique is employed in this study (Craig 1968).

3. ILLUSTRATIVE EXAMPLE

A jacket-type offshore structure as shown in Fig. 2 is chosen to demonstrate the applicability of the proposed technique for structural identification problems. The mass density and the elastic modulus of all members of baseline are 8000kg/m^3 and 2.1×10^{11}N/m. The areas and the moments of inertia of the cross-sectional areas of vertical, diagonal and horizontal members are (0.4m^2, 0.12m^4), (0.1m^2, 0.03m^4), and (0.02m^2, 0.002m^4), respectively. It is assumed that the unknown SSF's for the elements of the structure are between 0.5 and 1.5. The mode shapes are assumed to be measured only at 10 test DOF's, which include the displacements in x- and y-directions at 5 nodes of the internal-substructure; note that the rotational displacements are not included.

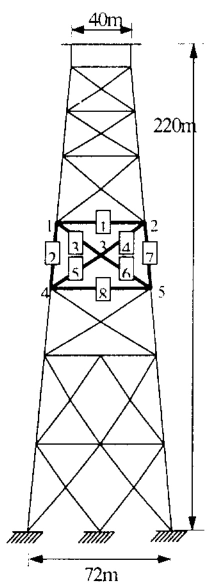

Fig. 2 Example structure

3.1 Input Patterns to BPNN

For an efficient training process, an appropriate number of modes as input to BPNN are selected. It is assumed that the first six modes of the internal-substructure at test DOF's are available in this study. The natural frequencies and mode shapes of the reference structure, in which all the SSF's are unity, are shown in Fig. 3. The fractional MSE distribution in the first six modes calculated for the reference state are shown in Fig. 4. Fig. 4 shows that the vertical elements such as 2 and 7 are carrying large fractions of the strain energy especially. It means that the modes contain

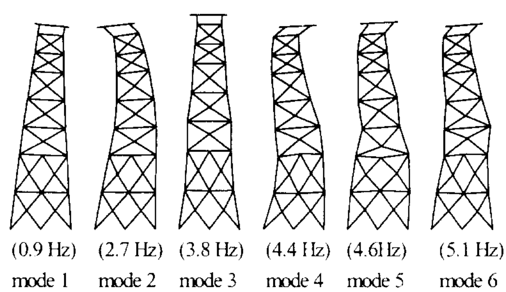

Fig. 3 First six mode shapes of example structure

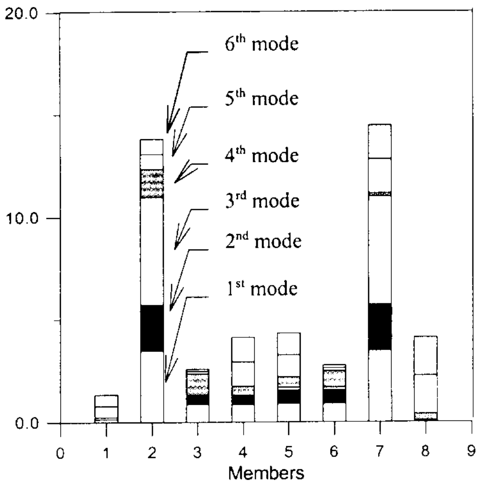

Fig. 4 Fractional modal strain energy distribution (%) of the reference structure

more information concerning the vertical elements than the others. On the other hand, the MSE coefficients for the horizontal elements 1 and 8 are relatively small for all the modes, which indicates that the SSF estimation for the horizontal elements may not be effective.

3.2 Training Patterns and Testing Patterns

For generation of training patterns using the Latin hypercube sampling, 21 sampling points are selected between 0.5 and 1.5 with an equal interval of 0.05 for each SSF in the internal substructures, assuming each SSF is uniformly distributed, while 11 sampling points between 0.5 and 1.5 are taken with an interval of 0.1 for the SSF's in the external substructures. Finer sampling has been taken for the internal substructure than the external substructure, since the purpose of this study is to identify the SSF's in the internal substructure. Consequently, the number of possible sample cases is 231(=21×11), which is not judged to be enough to represent the system adequately. Hence, eight iterations of the sampling process are taken, which results in 1848 sample cases. The elapse time for generating whole training data set is about 80 sec by the DEC Alphastation 200[4/233]. For the cases of testing patterns, the sampling points for the internal substructure are taken as the same to the training data, however the number of the sampling points for the external substructures is taken to be 10 in the range between 0.55 and 1.45 with an interval of 0.1. The difference in sampling is imposed, because the real testing patterns are not necessarily the same with the training patterns. Thus, the number of possible sample cases for testing is 210(21×10).

The patterns are generated by computing the natural frequencies and mode shapes using the CMS method. The training and testing data set for the noise-free and the 3% noise cases are prepared. The training data set is shown in Table 1.

3.3 Learning of Neural Network

It is important to choose the proper network size. In general, it is not straight forward to determine the best size of the networks for a given system. It may be found through trial and error process using knowledge about the system. A four-layer neural network as shown in Fig. 5 is selected for the present example. The numbers of neurons in the input, the first hidden, the second hidden and the output layer are 32, 20, 13, and 8, respectively. Numerical investigations show that small changes in the numbers of the neurons in the hidden layers have little effect on the estimation results.

Table 1 Training data set

Pattern 1	Input pattern without noise $(f_i,\ \tilde{\varphi}_{jk})$						
	0.878 2.608 3.736 4.250	0.530 0.460 -0.011 0.068	0.509 0.458 0.085 0.070	0.434 0.457 0.036 -0.262	....	0.104 -0.023 -0.452 0.205	-0.068 0.028 -0.403 -0.237
	Input pattern with 3% noise in RMS						
	0.891 2.772 3.793 4.166	0.550 0.469 -0.011 0.063	0.504 0.450 0.083 0.072	0.428 0.458 0.035 -0.250	....	0.102 -0.024 -0.455 0.203	-0.066 0.027 -0.407 -0.241
	Output pattern (SSF's) 0.60 1.50 0.50 1.25 1.75 0.60 1.35 1.35						
⋮							
Pattern 1848	Input pattern without noise $(f_i,\ \tilde{\varphi}_{jk})$						
	0.884 2.618 3.744 4.273	0.520 0.449 -0.012 0.003	0.512 0.459 0.076 0.088	0.429 0.450 0.041 -0.295	....	0.106 -0.022 -0.452 0.218	-0.069 0.029 -0.402 -0.277
	Input pattern with3% noise in RMS						
	0.866 2.576 3.802 4.102	0.498 0.437 -0.012 0.003	0.520 0.462 0.077 0.087	0.462 0.455 0.040 -0.294	....	0.108 -0.021 -0.430 0.223	-0.072 0.027 -0.403 -0.283
	Output pattern (SSF's) 1.10 1.40 0.80 0.75 1.00 1.20 1.50 1.45						

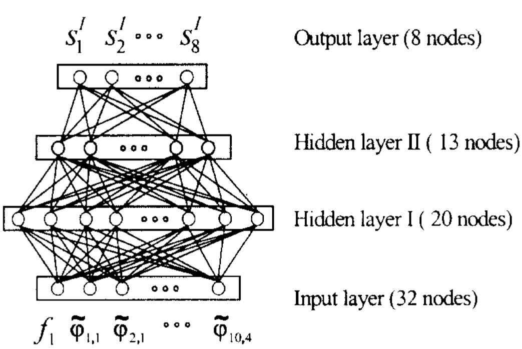

Fig. 5 Backpropagation neural network

The four-layer neural network is trained using 1,848 training patterns by the standard BP algorithm. The training process took about 2,000 iterations (epochs) to learn the pattern representation within tolerance accuracy, in which the elapse time is about 675 sec by an Alpastation computer system. One epoch means that all the 1,848 training patterns are used once for training. The tested outputs are listed in Table 2. Fig. 6 shows the averages of

Table 2 Testing data set

Pattern 1	Input pattern $(f_i, \tilde{\varphi}_{ji})$ with 3% noise						
	0.905 2.616 3.898 4.393	0.512 0.416 -0.018 0.119	0.517 0.450 0.034 0.056	0.440 0.473 -0.003 -0.224	....	0.087 -0.029 -0.360 0.279	-0.105 0.034 -0.458 -0.275
	Actual output 1.10 0.90 1.38 1.31 0.89 1.40 1.21 1.07						
	Target output (SSF's) 1.20 0.80 1.35 1.30 0.95 1.40 1.15 1.00						
	Relative error* (%) 8.51 12.67 1.89 1.08 6.29 0.02 4.99 6.52						
⋮							
Pattern 201	Input pattern $(f_i, \tilde{\varphi}_{ji})$ with 3% noise						
	0.816 2.625 3.393 4.082	0.513 0.439 -0.020 0.055	0.520 0.470 0.065 0.184	0.440 0.461 0.029 -0.204	....	0.111 -0.009 -0.434 0.277	-0.070 0.027 -0.379 -0.234
	Actual output 0.98 1.13 1.31 0.67 0.99 0.93 0.84 1.05						
	Target output (SSF's) 0.85 1.10 1.30 0.60 0.85 0.90 0.80 0.80						
	Relative error (%) 15.2 2.94 0.83 12.3 16.5 3.51 4.53 31.1						
	Average relative errors of each element for all the testing patterns 23.6 10.2 9.32 12.3 17.2 14.1 10.1 29.3 Average error for 8 elements = 15.76 %						
	*Note : Relative error(%) $= 100 \times \frac{\lvert Atual\ ouput - Target\ out \rvert}{Target\ output}$						

the relative errors in the estimated SSF's for various cases with different number of modes included in the input patterns. It can be found that the accuracy of the estimation improves with increasing number of the modes included until the 6^{th} modes.

Table 3 and Fig. 7 show the tested results for three cases with different noise levels in the training and testing data set. The average relative error of the tested outputs for the noise-free testing data, after the network is trained using the noise-free training data set, is 12.9%. But, the error for the 3% noise testing data using the same network is 23.3%. The result implies that the measurement error causes deterioration in the estimation. On the other hand, when the network is trained using the 3% noise training data set, the average relative error of the tested outputs for the 3% noise testing data is obtained as 15.8%, which is smaller than the average error of the test output (23.3%) using the noise-free training

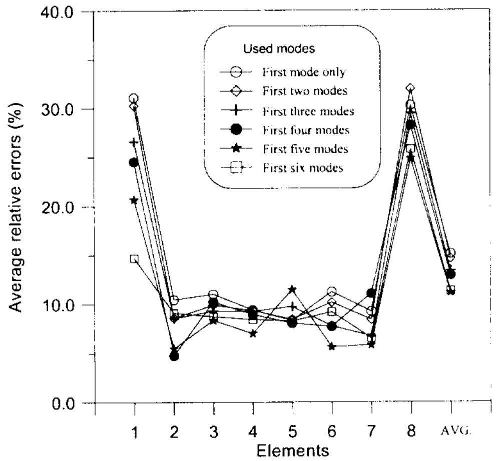

Fig. 6 Average estimation errors(%) for different modes used in input patterns (for testing data set without noise)

Table 3 Estimation errors(%) for different noise injection

Noise levels in RMS		in testing data		
		0%	3%	5%
in	0%	2.9	23.3	33.4
training	3%	15.2	15.8	17.6
data	5%	15.6	16.8	16.9

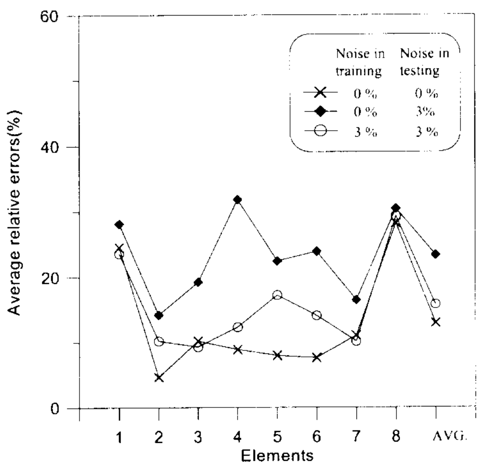

Fig. 7 Estimation error(%) for different noise injection learning

data. Fig. 8 is the learning curves to depict how the noise injection learning works. It is found that average relative error for the training case with 3% noise is smaller than that for the case without noise injection. This indicates that it is desirable to use the 3% noise data for training, if the measurement error is expected to be 3%. As anticipated in the previous section, the estimation errors of horizontal elements 1 and 8 are larger than those of the others.

4. CONCLUSIONS

For the assessment of structural integrity, the neural network-based structural identification is applied to the estimation of the parameters of offshore structures. The substructuring technique and the concept of submatrix scaling factor are employed to reduce the number of unknown parameters for local identification. The proposed neural network-based method does not require any complicated formulation. Particularly the conventional approaches can not apply to substructural identification directly without any model reduction of a system. This approach depends

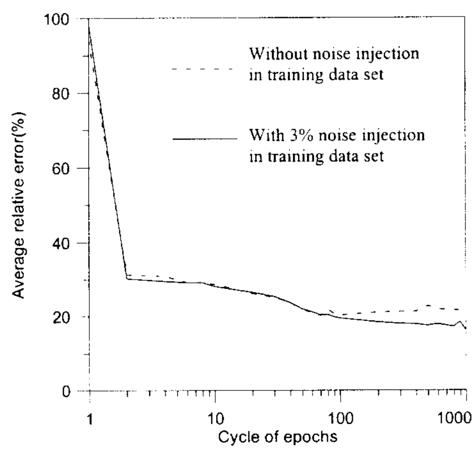

Fig. 8 Learning curves without and with noise injection levels.

upon how well and how compactly the training patterns represent the relationship between structural parameters and modal information. The Latin hypercube sampling and the fixed-interface-component-mode-synthesis (CMS) method provide a simple way to obtain such a training set.

A numerical example analysis on a jacket-type offshore structure is presented to demonstrate the effectiveness of the method. The average relative estimation error for the case with 3% noise testing data set is found to be about 16%. It has been found that the estimated results for the elements with larger MSE coefficients are better than those associated with smaller MSE coefficients.

ACKNOWLEDGEMENT

The authors would like to thank Korea Research Institute of Standards and Science (KRISS), and the Korea Science and Engineering Foundation (KOSEF) for their financial support for this study.

REFERENCES

1. Craig, R. R., Jr. and Bampton, M. C. C. (1968). "Coupling of Substructures for Dynamic Analysis", *AIAA Journal*, Vol. 6, No. 7, pp.1313~1319.
2. Ghanem, R. and Shinozuka, M. (1995). "Structural-System Identification I : Theory", *J. of Engineering Mechanics*, ASCE, Vol. 121, No. 2, pp.255~264.
3. Haykin, S. (1994). *Neural Networks-A Comprehensive Foundation*, Macmillan College Publishing Company, New York
4. Hong, K-S. and Yun, C-B. (1993). "Improved Method for Frequency Domain Identification of Structures", *Eng. Struct.*, Vol. 15, No. 3, pp.179~188.
5. Hush, D. R. and Horne, B. G. (1993). "Progress in Supervised Neural Networks", *IEEE Signal Processing Magazine*, pp.8~39.
6. Koh, Chan G., et al. (1991). "Estimation of Structural Parameters in the Time Domain : A Substructure Approach", *Earthquake Engineering and Structural Dynamics*, Vol. 20, pp.787~801.
7. Lim, T.W. (1990). "Submatrix Approach to Stiffness Matrix Correction Using Modal Test Data", *AIAA Journal*, Vol. 28, No. 6. pp.1123~1130.
8. Lim, T.W. (1991). "Structural Damage Detection Using Modal Test Data", *AIAA Journal*, Vol 29, No. 12. pp.2271~2274.
9. Oreta, Andres W. C. and Tanabe, Tada-aki. (1976). "Element Identification of Member Properties of Framed Structures", *J. of Structural Engineering*, ASCE, Vol. 120, No. 7, pp.1961~1976.
10. Pandey, P. C. and Barai, S. V. (1995), "Multilayer Perceptron in Damage Detection of Bridge Structures", *Comput. Struct.*, 54 (4), pp.597~608.
11. Press, W., Teukolsky, S.A., Vetterling, W. T. and Flannery, B. P. (1992). *Numerical recipes in C-The art of scientific computing.* Cambridge University Press, New York, p.315.
12. Tsou, Poyu and Shen M.-H. Herman. (1994). "Structural Damage Detection and Identification Using Neural Networks", *AIAA Journal*, Vol.32, No.1, pp.176~183
13. Wu, X., Ghaboussi, J., and Garrett, J.H. Jr. (1992). "Use of Neural Networks in Detection of Structural Damage", *Comput. Struct.*, 42(4), pp.649~659.
14. Yun, C-B. and Lee, H-J. (1995). "Damage estimation of structures incorporating substructural identification", *Proceedings of APSSRA, Tokyo, Japan.*

(접수일자 : 1998. 11. 7)